On the Motion of a Particle in the Kerr Metric

Motta J. Llanos C. Cordoba A. Niño D.
National University of Colombia, Bogotá Campus

Abstract

In this work, we solved the geodesic equations in the Kerr metric using the Bulirsch-Stoer numerical method for the general case and the Runge-Kutta method for the equatorial plane. We implemented a code to calculate particle trajectories and analyzed their behavior. When comparing with the fourth-order Runge-Kutta method, we found that Bulirsch-Stoer offers better numerical stability. However, it is still not physically exact since undefined values (NaN) persist in the general case. For the equatorial plane case, a solution closer to the expected behavior was achieved. Nevertheless, its comparison with the analytical expression of the particular case $L = aE$, given by Chandrasekhar, suggests that the code requires further refinement. Additionally, the graphical representation of the analytical solution still needs corrections. The obtained results allow us to visualize how the Kerr metric affects particle motion and evaluate the precision of our implementation.

Introduction

In 1795, Pierre-Simon Laplace hypothesized, based on Newtonian gravity, that sufficiently massive objects could possess gravitational fields so intense that their escape velocities might exceed the speed of light [1]. Over a century later, Einstein's 1915 general theory of relativity fundamentally redefined gravity as spacetime curvature, with his field equations implicitly predicting the existence of spacetime singularities: regions of infinite curvature where classical physics breaks down [2]. Shortly afterward, Karl Schwarzschild derived the first exact solution to Einstein's equations, describing the spacetime geometry exterior to a static, spherically symmetric massive object [3]. Decades later, Roy Kerr expanded this work by deriving a solution for rotating compact masses [4], a metric now recognized as fundamental for modeling astrophysical black holes.

While analytical solutions for geodesic motion in Kerr spacetime were established by the mid-20th century [5][6], their mathematical complexity limits its interpretability. Therefore, numerical methods have become indispensable for exploring orbital dynamics, investigating chaotic behavior, and modeling phenomena such as extreme mass-ratio inspirals. These computational approaches complement analytical work and enable the study of scenarios inaccessible to closed-form solutions.

In this study, we implemented numerical schemes to solve the geodesic equations in Kerr spacetime and validated our results against known analytical solutions (case $L = aE$). This dual approach ensures methodological rigor while deepening our understanding of spacetime geometry's interaction with test particle dynamics. Furthermore, this work serves as a bridge to advanced research topics such as gravitational wave physics and the relativistic two-body problem.

Procedure

The metric in Boyer-Lindquist coordinates for Kerr spacetime can be described by:

$$d\tau^2 = \left(1 - \frac{r_s}{r}\right) dt^2 - \left(\frac{r^2}{r^2 - r_s r + a^2}\right) dr^2 - \left(r^2 + a^2 + \frac{r_s a^2}{r}\right) d\phi^2 + \frac{2 r_s a}{r} dt d\phi$$

Where r_s is the Schwarzschild radius (with $r_s = 2M$ in geometric units) and a represents the black hole's angular momentum parameter.

The evolution equations derived from energy E and angular momentum L conservation laws are:

$$\dot{t} = \frac{1}{a^2 + r^2 - r_s r}\left[E\left(r^2 + a^2 + \frac{r_s a^2}{r}\right) - L\left(\frac{r_s a}{r}\right)\right],$$

$$\dot{\phi} = \frac{1}{a^2 + r^2 - r_s r}\left[E\left(\frac{r_s a}{r}\right) + L\left(1 - \frac{r_s}{r}\right)\right],$$

$$r^2 \dot{r}^2 = r^2 E^2 + \frac{r_s}{r}(aE - L)^2 + (a^2 E^2 - L^2) - (a^2 + r^2 - r_s r). \quad (1)$$

For the equatorial plane case, we proceeded to solve using Runge-Kutta with some modifications mentioned later in the text.

Additionally, we used other equations formulated by Chandrasekhar [5], studying unbound behavior in the $\theta = \pi/2$ coordinate (equatorial plane):

$$
\begin{aligned}
\rho^4 \dot{r}^2 &= \left[(r^2+a^2)E - aL_z\right]^2 - \Delta C, \\
\rho^4 \dot{\theta}^2 &= -\left(aE\sin\theta - L_z \csc\theta\right)^2 + C, \\
\rho^2 \dot{t} &= \frac{1}{\Delta}\left[(r^2+a^2)E - 2aMrL_z\right], \\
\rho^2 \dot{\phi} &= \frac{1}{\Delta}\left[2aMrE + (\rho^2 - 2Mr)L_z \csc\theta\right].
\end{aligned} \tag{2}
$$

For general particle motion, we initially implemented the Runge-Kutta 4 solution, later switching to the Burlisch-Stoer method.

Numerical Solution: Fourth-Order Runge-Kutta Method (RK4)

The fourth-order Runge-Kutta method (RK4) is one of the most widely used schemes for integrating ordinary differential equations due to its precision and computational efficiency. In this work, we implemented RK4 for the numerical evolution of geodesic equations in the Kerr metric.

This scheme evaluates the derivative at four distinct points within the integration interval, achieving better approximation compared to lower-order methods like Euler or RK2.

For the numerical evolution of particle motion equations in the Kerr metric, we applied RK4 to the differential equations of coordinates (t, r, θ, ϕ). We defined a data structure storing the system state, enabling efficient time stepping.

The integration procedure consists of:

1. Calculating coefficients k_1, k_2, k_3, k_4 using evolution equations.
2. Combining coefficients according to RK4 rules to obtain the new system state.
3. Repeating the process for each time step until completing the desired trajectory.

Although RK4 is robust and widely used, numerical instabilities or truncation error accumulation may occur in certain regions of a rotating black hole's ergosphere. The following section compares its performance with the Burlisch-Stoer method, showing differences in stability and integration precision.

Numerical Solution: Burlisch-Stoer Method Without Constraints

To improve code stability in ergosphere regions, we manually implemented the Burlisch-Stoer method, which "is the best-known way to obtain high-precision solutions to ordinary differential equations with minimal computational effort" [7].

For implementation, we used the same evolution equations, defining three essential functions. One, based on the modified midpoint method, uses:

$$
\begin{aligned}
z_0 &= y(x), \\
z_1 &= z_0 + h\, f(x, z_0), \\
z_{m+1} &= z_{m-1} + 2h\, f(x + mh, z_m) \quad \text{for } m = 1, 2, \ldots, n-1,
\end{aligned}
$$

with final estimation

$$
y(x+H) \approx y_n = \frac{1}{2}\left[z_n + z_{n-1} + h\, f(x+H, z_n)\right],
$$

where $h = H/n$. These equations advance an $n+1$-sized vector (including initial conditions) through n substeps, using a data structure called *state* grouping variables r, θ, t, and ϕ.

Subsequently, Richardson extrapolation is applied to the midpoint method:

$$
\text{temp}[i] = \frac{2^{2j} \cdot \text{temp}[i+1] - \text{temp}[i]}{2^{2j} - 1},
$$

where j is the extrapolation level and i the estimate index. A copy of the *state* vector is made in a vector called `temp`, and through two loops (one for j and another for i), successive estimates are combined. In each iteration, `temp[i]` is updated with a more precise estimate, ensuring that `temp[0]` ultimately represents the refined solution. This procedure eliminates the principal error term proportional to h^2 by combining estimates with different step sizes.

Comparing this method with fourth-order Runge-Kutta yielded fig. 1.

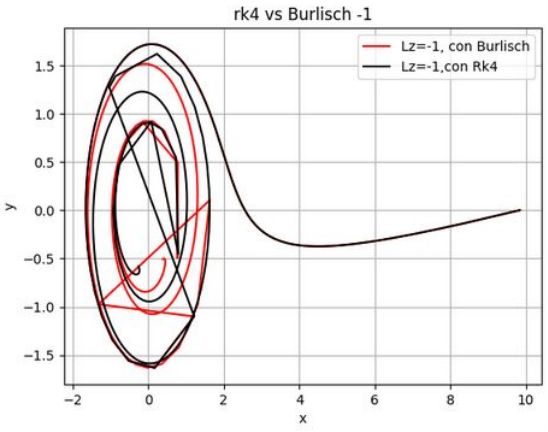

Figure 1: *RK4 vs. Burlisch-Stoer with $L_z = -1$, 10000 steps*

In fig. 1, both methods initially yield identical results, but upon entering the ergosphere region (fig. 2), Burlisch-Stoer produces smoother trajectories with fewer abrupt jumps, though some discontinuities remain apparent.

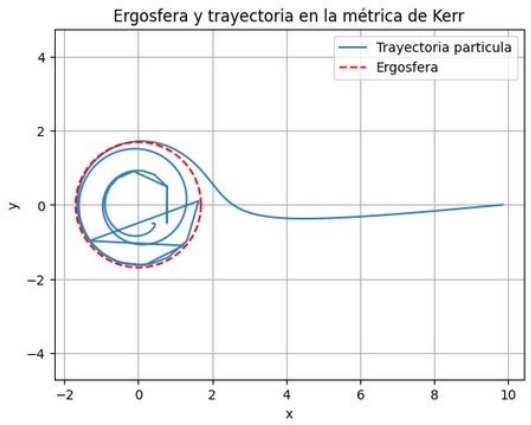

Figure 2: *Ergosphere vs. particle trajectory with Burlisch-Stoer and* $L_z = -1$

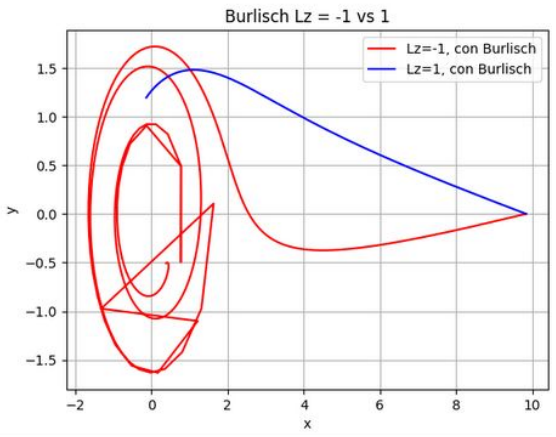

Figure 3: *Trajectory comparison with angular momentum equal to 1 and -1*

Finally, we attempted to eliminate NaN values (discussed next) but were unsuccessful, leaving this as future work.

The NaN Problem

During integration, particularly in bounded orbit regimes ($E < 1$) with high angular momentum values, undefined values (NaN) emerged. This issue arises from sign changes in the effective potential $R(r)$, which must remain positive for physical solutions.

To mitigate this, we implemented several approaches: integration method refinements and dynamic time step adjustments in critical regions. However, the solution emerged by introducing a function that inverts the potential sign at inflection points, analogous to choosing the positive square root branch in the radial evolution equation.

While these strategies improved equatorial plane integration, the general case problem remains for future work.

Analysis

Our results demonstrate that the Burlisch-Stoer method offers significant advantages for integrating geodesic equations within the Kerr metric. Compared to RK4, both methods agree in regions distant from the event horizon, but Burlisch-Stoer generates smoother trajectories with fewer numerical jumps in the ergosphere due to its error-reducing extrapolations.

Another key aspect is visualizing how angular momentum parameter L_z affects trajectories, showing marked differences between $L_z = 1$ and $L_z = -1$ cases (fig. 3). Our computational framework enables future extensions for analyzing chaotic orbits or gravitational wave emissions.

For the equatorial plane case (where NaN issues were resolved), we obtained:

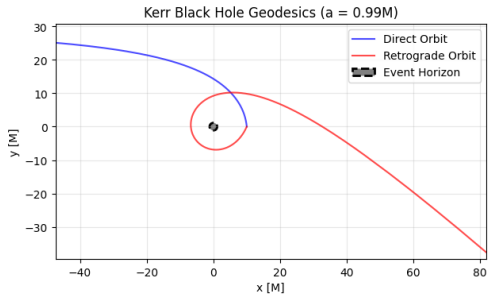

Figure 4: *Geodesic trajectory with* $E = 1.01$, $L_+ = 5$ *and* $L_- = -5$ *(co-rotating and counter-rotating escape cases).*

fig. 4 shows expected behavior: for $E > 1$ and chosen angular momentum parameters, the particle escapes gravitational attraction.

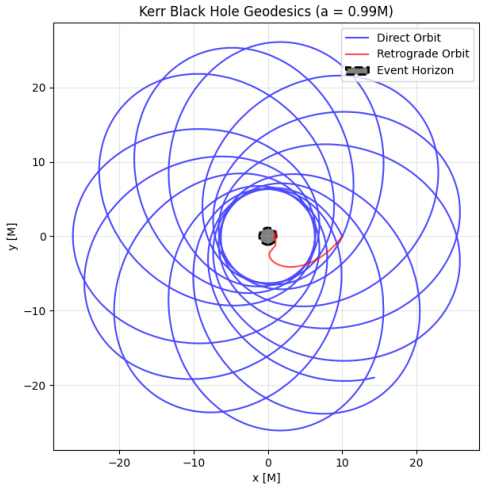

Figure 5: *Stable bounded orbit with $E = 0.97$, $L_+ = 3.5$ and $L_- = -3.5$ (co-rotating case).*

fig. 5 displays a stable orbit since $E < 1$ and the effective potential's first derivative is negative.

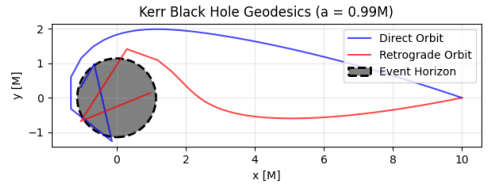

Figure 6: *Trajectory where particle falls through the horizon, with $E = 0.97$, $L_+ = 1$ and $L_- = -1$.*

fig. 6 demonstrates horizon crossing for $E < 1$ and critical angular momentum.

We compared numerical results with Chandrasekhar's analytical solutions for $L = aE$ [5]:

$$\tau = \frac{1}{E^2-1}\left[\sqrt{(E^2-1)r^2+2Mr-a^2}\right.$$
$$\left.+\frac{1}{\sqrt{1-E^2}}\sin^{-1}\left(\frac{(M+(E^2-1)r)}{(-a^2(1-E^2)+M^2)^{1/2}}\right)\right].$$

Angular coordinate:

$$\phi = \frac{1}{a(u_+ - u_-)}$$
$$\left\{\ln\left[2E\sqrt{E^2\xi_+^2+2(M-a^2u_+)\xi_+ - a^2}\right.\right.$$
$$\left.+2E^2\xi_+ + 2(M-a^2u_+)\right]$$
$$-\ln\left[2E\sqrt{E^2\xi_-^2+2(M-a^2u_-)\xi_- - a^2}\right.$$
$$\left.\left.+2E^2\xi_- + 2(M-a^2u_-)\right]\right\}.$$

Implementing these yielded:

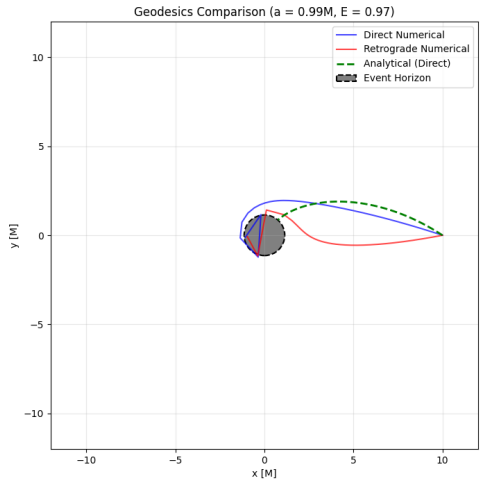

Figure 7: *Analytical vs. numerical trajectories with $a = 0.99$, showing discrepancies likely due to implicit solution implementation.*

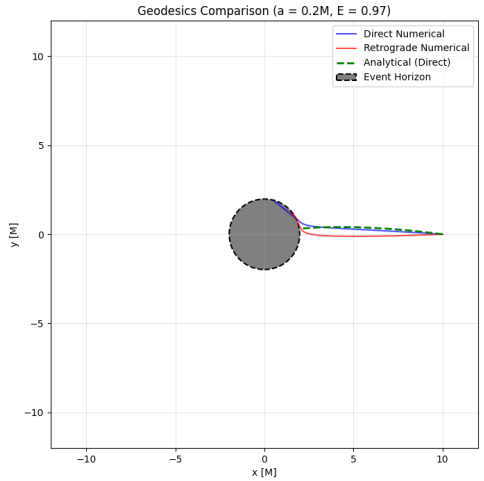

Figure 8: *Analytical vs. numerical trajectories with $a = 0.2$, showing closer agreement.*

Conclusions

- Efficient numerical implementation for Kerr metric geodesic trajectories was achieved, validated against analytical solutions and numerical comparisons.
- Burlisch-Stoer proved robust for ergosphere integration, outperforming RK4 in stability.
- Angular momentum parameter L_z significantly affects trajectories, with distinct co-rotating ($L_z = 1$) and counter-rotating ($L_z = -1$) behaviors.
- Our computational framework enables future studies of chaotic orbits and gravitational wave emissions.
- This work establishes foundations for advanced relativistic particle dynamics studies near rotating black holes.

References

[1] S. W. Hawking and G. F. R. Ellis. *The Large Scale Structure of Space-Time*. Cambridge University Press, 1973.

[2] Albert Einstein. "Die Feldgleichungen der Gravitation". In: *Sitzungsberichte der Preussischen Akademie der Wissenschaften zu Berlin* (1915), pp. 844–847.

[3] Karl Schwarzschild. "Über das Gravitationsfeld eines Massenpunktes nach der Einsteinschen Theorie". In: *Sitzungsberichte der Königlich Preussischen Akademie der Wissenschaften* (1916), pp. 189–196.

[4] Roy P. Kerr. "Gravitational field of a spinning mass as an example of algebraically special metrics". In: *Physical Review Letters* 11.5 (1963), p. 237.

[5] Subrahmanyan Chandrasekhar. *The Mathematical Theory of Black Holes*. Oxford University Press, 1983.

[6] Brandon Carter. "Global structure of the Kerr family of gravitational fields". In: *Physical Review* 174.5 (1968), p. 1559.

[7] William H. Press et al. *Numerical Recipes: The Art of Scientific Computing*. 3rd. Cambridge: Cambridge University Press, 2007. ISBN: 978-0-521-88068-8.